Direct Evidence for Specific Interactions of the Fibrinogen αC-Domains with the Central E Region and with Each Other†

Rustem I. Litvinov,*,‡ Sergiy Yakovlev,§ Galina Tsurupa,§ Oleg V. Gorkun,|| Leonid Medved,*,§ and John W. Weisel‡

Department of Cell and Developmental Biology, University of Pennsylvania School of Medicine, Philadelphia, Pennsylvania 19104-6058, Center for Vascular and Inflammatory Diseases and Department of Biochemistry and Molecular Biology, University of Maryland School of Medicine, Baltimore, Maryland 21201, and Department of Pathology and Laboratory Medicine, University of North Carolina, Chapel Hill, North Carolina 27599-7525

Received May 16, 2007; Revised Manuscript Received June 5, 2007

ABSTRACT: The carboxyl-terminal regions of the fibrinogen Aα chains (αC regions) form compact αC-domains tethered to the bulk of the molecule with flexible αC-connectors. It was hypothesized that in fibrinogen two αC-domains interact intramolecularly with each other and with the central E region preferentially through its N-termini of Bβ chains and that removal of fibrinopeptides A and B upon fibrin assembly results in dissociation of the αC regions and their switch to intermolecular interactions. To test this hypothesis, we studied the interactions of the recombinant αC region (Aα221−610 fragment) and its subfragments, αC-connector (Aα221−391) and αC-domain (Aα392−610), between each other and with the recombinant $(B\beta 1-66)_2$ and $(\beta 15-66)_2$ fragments and NDSK corresponding to the fibrin(ogen) central E region, using laser tweezers-based force spectroscopy. The αC-domain, but not the αC-connector, bound to NDSK, which contains fibrinopeptides A and B, and less frequently to desA-NDSK and $(B\beta 1-66)_2$ containing only fibrinopeptides B; it was poorly reactive with desAB-NDSK and $(\beta 15-66)_2$ both lacking fibrinopeptide B. The interactions of the αC-domains with each other and with the αC-connector were also observed, although they were weaker and heterogeneous in strength. These results provide the first direct evidence for the interaction between the αC-domains and the central E region through fibrinopeptide B, in agreement with the hypothesis given above, and indicate that fibrinopeptide A is also involved. They also confirm the hypothesized homomeric interactions between the αC-domains and display their interaction with the αC-connectors, which may contribute to covalent cross-linking of α polymers in fibrin.

Fibrinogen is a blood plasma protein involved in a number of (patho)physiological processes such as hemostasis, fibrinolysis, inflammation, angiogenesis, wound healing, and neoplasia (*1*, *2*). This polyfunctionality is due to the complex structure of fibrinogen molecules that have multiple binding sites, either constitutively open or exposed after precise enzymatic cleavage and/or conformational rearrangement. The ability to polymerize upon the action of thrombin is the unique property of fibrinogen that mainly determines its physiological significance.

Structurally, fibrinogen is a 45 nm long elongated dimer composed of three pairs of nonidentical polypeptide chains, designated Aα, Bβ, and γ (Figure 1). The N-termini of the six chains, cross-linked by a cluster of disulfide bonds, form a central part, hence named the "N-terminal disulfide knot" (*3*). The C-termini of Bβ and γ chains form globular modules on each end of the molecule separated from the central part by triple-helical coiled coils (*4*, *5*). The C-terminal portions of the Aα chains extend from the coiled coils and form αC regions, each comprising approximately two-thirds of the Aα chain (residues 221−610 in human fibrinogen). The αC region was shown to consist of a relatively compact C-terminal portion named the αC-domain (residues 392−610) attached to the bulk of the molecule via a flexible tether named the αC-connector (residues 221−391) (*6*−*8*).

Functionally, αC regions of fibrinogen are implicated with a number of important molecular interactions, including those in fibrin assembly, which are not yet well understood. Fibrin assembly starts when thrombin converts fibrinogen into fibrin monomer by cleaving a short N-terminal portion of the Aα chains called fibrinopeptide A (FpA).[1] Then, the newly formed desA-fibrin monomers spontaneously self-assemble into two-stranded oligomeric protofibrils. Once the protofibrils reach a critical length, they aggregate laterally to form fibers, which are organized into the branched network, a fibrin clot. After fibrin has partially formed, thrombin cleaves

† This work was supported by Grants HL-30954 (to J.W.W.) and HL-56051 (to L.M.) from the National Institutes of Health.

* To whom correspondence should be addressed. R.I.L.: Department of Cell and Developmental Biology, University of Pennsylvania School of Medicine, 421 Curie Blvd., 1040 BRB II/III, Philadelphia, PA 19104-6058; telephone, (215) 898-9141; fax, (215) 898-9871; e-mail, litvinov@mail.med.upenn.edu. L.M.: Center for Vascular and Inflammatory Diseases, Department of Biochemistry and Molecular Biology, University of Maryland School of Medicine, 800 W. Baltimore St., Baltimore, MD 21201; telephone, (410) 706-8065; fax, (410) 706-8121; e-mail, Lmedved@som.umaryland.edu.

‡ University of Pennsylvania School of Medicine.

§ University of Maryland School of Medicine.

|| University of North Carolina.

10.1021/bi700944j CCC: $37.00
Published on Web 07/13/2007

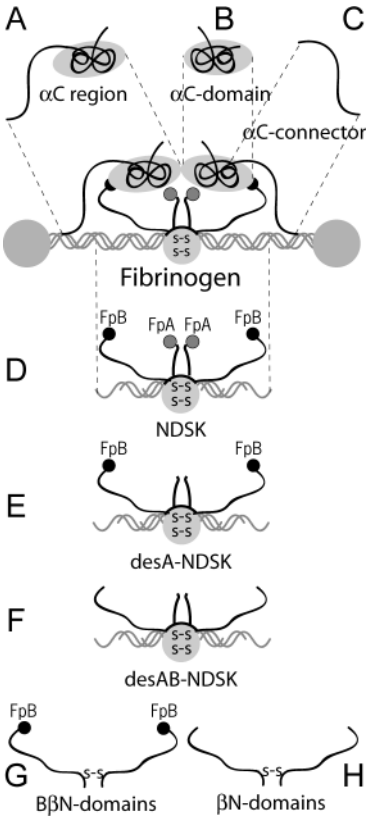

FIGURE 1: Cartoon of fibrinogen and fibrin(ogen) fragments used in this study. Panels A−C show the αC region fragment corresponding to the C-terminal portion of the fibrinogen Aα chain (residues Aα221−610) and its subfragments, the αC-domain (residues Aα392−610) and αC-connector (residues Aα221−391), respectively. Panels D−F show NDSK [N-terminal disulfide knot (*3*)], a fragment from the central part of fibrinogen containing both FpA and FpB, desA-NDSK with FpA cleaved but with FpB remaining, and desAB-NDSK with both FpA and FpB cleaved, respectively. Panel G shows the recombinant fibrinogen $(B\beta 1-66)_2$ fragment consisting of two Bβ N-domains formed by the N-terminal portions of the fibrinogen Bβ chains. Panel H shows the recombinant fibrin fragment $(\beta 15-66)_2$, including two βN-domains devoid of FpB. The gray and black circles on the ends represent fibrinopeptides A (FpA) and B (FpB), respectively. The gray circle in the center with double designations "S−S" inside represents a cluster of disulfide bonds.

fibrinopeptide B (FpB) from the N-terminal portions of the Bβ chains (*9*, *10*); this reaction gives rise to additional intermolecular interactions that reinforce the clot (*11*, *12*). Finally, the mature clot is stabilized by covalent cross-linking of specific amino acids by a transglutaminase, factor XIIIa (*1*, *2*, *13*, *14*). The notion that αC regions are involved in fibrin formation is based on three clusters of data. (i) Clot formation is slowed, and the clot structure is perturbed when αC regions are removed from fibrinogen either proteolytically (*15*−*19*) or as a result of a natural and/or artificial genetic defect (*20*−*32*). (ii) Isolated αC fragments (*19*, *33*, *34*) or αC-specific antibodies (*35*, *36*) interfere with clot formation. (iii) αC regions polymerize and can be cross-linked by factor XIIIa, thus contributing to clot stability (*33*, *37*−*40*).

It has been hypothesized that in fibrinogen the αC-domains interact intramolecularly with each other and with the central E region via FpB, while during fibrin assembly, they dissociate following the FpB cleavage and switch from intra- to intermolecular interaction (*6*, *17*, *19*, *33*, *41*). Although this "intra- to intermolecular switch" hypothesis coherently accounts for the location of the αC-domains in fibrinogen and fibrin and suggests a possible mechanism for the exposure of their multiple binding sites upon conversion of fibrinogen to fibrin, it is not universally accepted (*42*). The major reason for the lack of consensus is that this hypothesis is based mainly on low-resolution data obtained by electron microscopy. To test this hypothesis, we used laser tweezers-based force spectroscopy to examine binding specificity and measure the binding strength of fibrin(ogen) fragments, representing the full-length αC region or its constituents, αC-domain and αC-connector, as well as the fragments, bearing N-terminal portions of Bβ chains (Bβ N-domains) (Figure 1). The laser tweezers technique that enables quantification of individual protein−protein interactions is based on the ability of the optical system to measure the rupture forces of two surface-bound protein molecules (*43*−*45*). Recently, we used this technique to examine the role of various molecular interactions, other than those mediated by αC-domain, in fibrin polymerization (*41*, *46*, *47*). Here we provide direct evidence of the specific binding of the isolated αC-domain to the FpB-containing fibrinogen Bβ N-domains, but not to the fibrin βN-domains lacking FpB. In addition, we show that the αC-domains interact with each other, but their association is weaker than the αC−Bβ N binding.

MATERIALS AND METHODS

Recombinant Fibrin(ogen) αC Fragments. The recombinant αC fragment corresponding to the human fibrinogen αC region (residues Aα221−610) and its constituents, αC-connector (residues Aα221−391) and αC-domain (residues Aα392−610), were produced in *Escherichia coli*, purified, and refolded as described previously (*7*, *48*). The purity of all fragments was confirmed by SDS−PAGE; the fragments were concentrated to 1.0−2.0 mg/mL and kept at 4 °C.

Recombinant Fibrin(ogen) (B)βN-Containing Fragments and the Monoclonal Antibody. The recombinant $(B\beta 1-66)_2$ fragment mimicking the dimeric arrangement of the Bβ chains in fibrinogen, which form two Bβ N-domains (Figure 1G), was produced in *E. coli* and purified as described elsewhere (*49*). To produce the activated $(\beta 15-66)_2$ fragment, corresponding to fibrin βN-domains lacking FpB (Figure 1H), $(B\beta 1-66)_2$ was treated with thrombin and then purified as described previously (*49*). The purity of nonactivated and activated (B)βN-containing fragments was confirmed by SDS−PAGE. The anti-Bβ1−21 18C6 monoclonal antibody (*50*, *51*) was purchased from Accurate Chemicals (Westbury, NY).

NDSK Fibrin(ogen) Fragments. NDSK fragment, obtained by digestion of fibrin(ogen) with CNBr, is composed of two of each of the Aα1−51-, Bβ1−118-, and γ1−78-chains linked together by 11 disulfide bonds (*52*, *53*). Using the procedure described elsewhere (*46*, *52*), we prepared three variants of NDSK fragments: NDSK retaining both FpA and

[1] Abbreviations: FpA, fibrinopeptide(s) A; FpB, fibrinopeptide(s) B; NDSK, N-terminal disulfide knot; desA-NDSK, N-terminal disulfide knot with cleaved FpA; desAB-NDSK, N-terminal disulfide knot with cleaved FpA and FpB; SDS−PAGE, sodium dodecyl sulfate−polyacrylamide gel electrophoresis; HEPES, 4-(2-hydroxyethyl)-1-piperazineethanesulfonic acid; BSA, bovine serum albumin; mAb, monoclonal antibody.

FpB (Figure 1D) generated by CNBr cleavage of human plasma fibrinogen, desA-NDSK lacking FpA (Figure 1E) generated by CNBr cleavage of fibrin clotted with batroxobin, and desAB-NDSK lacking both FpA and FpB (Figure 1F) generated by CNBr cleavage of fibrin clotted with thrombin. Purified NDSK fragments were characterized by SDS−PAGE, dialyzed against 20 mM HEPES buffer (pH 7.4) containing 150 mM NaCl, and stored at −80 °C.

Coating Surfaces with Proteins. Surfaces coated with the interacting proteins were prepared basically as described previously (*41*, *44*, *46*). One of the interacting proteins was bound covalently to 5 μm spherical silica pedestals anchored to the bottom of a chamber. Pedestals coated with a thin layer of polyacrylamide were activated with 10% glutaraldehyde (1 h, 37 °C), washed thoroughly with 0.055 M borate buffer (pH 8.5), after which 1 mg/mL protein in 20 mM HEPES (pH 7.4) with 150 mM NaCl was inserted into the chamber and allowed to immobilize for 2 h at 4 °C. After the chamber had been washed with 20 volumes of the same buffer to remove the unbound protein, 2 mg/mL bovine serum albumin (BSA) in 0.055 M borate buffer (pH 8.5) with 150 mM NaCl was added as a blocker (1 h, 4 °C). In control experiments, the BSA-containing buffer was added right after glutaraldehyde activation followed by washing of the chamber. To convert Bβ N-domains to β N-domains on the surface, the immobilized Bβ N-domain-containing fragments were treated with human thrombin (1 unit/mL, 37 °C, 1 h), followed by washing of the chambers with 20 volumes of cold (4 °C) 100 mM HEPES (pH 7.4) containing 150 mM NaCl, 3 mM $CaCl_2$, 2 mg/mL BSA, and 0.1% (v/v) Triton X-100 ∼30 min before the measurements. All the procedures were performed at 0−4 °C, and the chambers containing protein-coated surfaces were stored at 4 °C and used within 3 h.

The other interacting protein was bound covalently to carboxylate-modified 1.87 μm latex beads using *N*-[3-(dimethylamino)propyl]-*N*′-ethylcarbodiimide hydrochloride (Sigma, St. Louis, MO) as a cross-linking agent (*46*). BSA (2 mg/mL) in 0.055 M borate buffer (pH 8.5) was used as a blocker. The protein-coated beads were freshly prepared, stored on ice, and used within 3 h. The surface density of all the proteins was at the point of surface saturation, since a further increase in the time of immobilization did not augment the maximal binding probability; nonetheless, the fraction of reactive molecules that have a conformation and orientation compatible with binding was indeterminate.

The Model System for Studying Protein−Protein Interactions. We used a laser tweezers-based model system to study interactions between two surface-bound proteins (*44*−*46*). Laser tweezers are an optical system that use laser light to trap and manipulate dielectric particles such as small latex beads (*43*, *54*, *55*). External forces applied to the trapped particle can be accurately measured because the angular deflection of the laser beam is directly proportional to the lateral force applied to the particle (*56*−*58*). This system permits the measurement of discrete rupture forces produced by surface-bound molecular pairs during repeated intermittent contact (*44*, *45*).

To study particular protein pairs, fibrin(ogen) fragments of interest were bound to pedestals and beads. In most cases, the αC region fragment and NDSK fragments were covalently bound to stationary pedestals anchored to the inner surface of a flow chamber, while the smaller proteins [αC-domain, αC-connector, $(B\beta 1-66)_2$, and $(\beta 15-66)_2$] were bound to the moving latex beads. In a number of experiments, the interacting proteins were immobilized on the opposite surfaces, which did not cause a difference in results. The suspension of protein-coated beads (10^7 per milliliter) in 100 mM HEPES buffer (pH 7.4) containing 150 mM NaCl, 3 mM $CaCl_2$, 2 mg/mL BSA, and 0.1% (v/v) Triton X-100 was then passed into the chamber. One of the latex beads was trapped by a focused laser beam and moved in an oscillatory manner so that the bead was intermittently in contact with a stationary pedestal. The tension produced when a protein on the latex bead interacted with a complementary molecule(s) on the anchored pedestal was sensed and displayed as a force signal that was proportional to the strength of protein−protein binding (*46*). Rupture forces from many interactions were collected and displayed as normalized force spectra histograms for each experimental condition. The binding experiments were performed at room temperature in 100 mM HEPES buffer (pH 7.4) containing 150 mM NaCl and 3 mM $CaCl_2$ with 2 mg/mL BSA and 0.1% (v/v) Triton X-100 added to reduce the level of nonspecific interactions.

Measurement of Binding Strength, Data Processing, and Data Analysis. The position of the optical trap and hence a protein-coated latex bead was oscillated in a triangular waveform at 1 Hz with a pulling velocity of 1.8 μm/s, which corresponded to a loading rate of 800 pN/s. Contact duration between interacting surfaces varied from 10 to 100 ms. Rupture forces were collected at 2000 scans per second (0.5 ms time resolution). The results of many experiments under similar conditions were averaged so that each rupture force histogram represented from 10^3 to 10^4 repeated contacts of more than 10 different bead−pedestal pairs. Individual forces measured during each contact−detachment cycle were collected into 10 or 5 pN wide bins. The number of events in each bin was plotted against the average force for that bin after normalizing for the total number of interaction cycles. The percentage of events in a particular force range (bin) represents the probability of rupture events at that tension. Optical artifacts observed with or without trapped latex beads produce signals that appeared as forces below 10 pN. Accordingly, rupture forces in this range were not considered when the data were analyzed. The rupture force histograms were fit empirically with multimodal Gaussian curves using Origin 7.5 (OriginLab Corp., Northampton, MA) to determine the position of a peak that corresponds to the most probable rupture force.

RESULTS

Interactions of the αC Region and Its Constituents with the (B)βN-Domains. To check directly whether the N-terminal portions of the fibrinogen Bβ chains bind to the C-terminal portions of the Aα chains, the recombinant $(B\beta 1-66)_2$ fragment containing two disulfide-linked Bβ N-domains[2] (Figure 1G) was exposed to the αC region fragment and its subfragments, comprising the αC-domain and αC-connector (Figure 1A−C). For the interactions of the αC

[2] For the sake of simplicity, the word "fragment" is often omitted hereafter and the dimeric (B)β N-domain-containing fragments, $(B\beta 1-66)_2$ and $(\beta 15-66)_2$, are called (B)β N-domains.

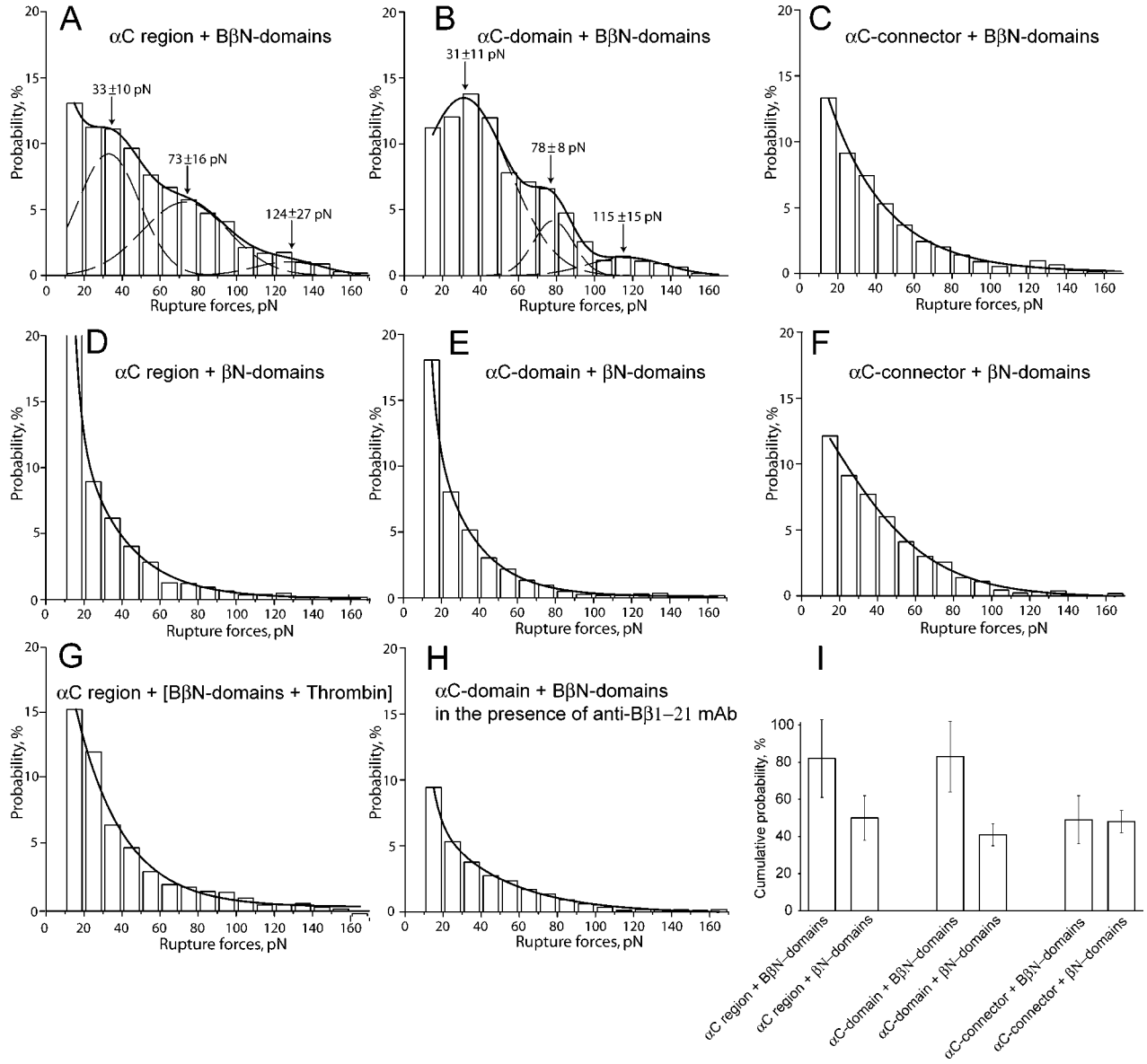

FIGURE 2: Panel of rupture force histograms demonstrating interactions of the recombinant fragment corresponding to the αC region and its subfragments, αC-connector and αC-domain, with the recombinant $(B\beta 1-66)_2$ and $(\beta 15-66)_2$ fragments corresponding to the fibrinogen BβN-domains and fibrin βN-domains, respectively. (A−C) Interactions of the BβN-domains with the αC region, αC-domain, and αC-connector, respectively. (D−F) Interactions of the βN-domains with the αC region, αC-domain, and αC-connector, respectively. (G) Interactions of the αC region with the BβN-domains treated with thrombin and thus converted to the βN-domains right on the surface. (H) Interactions of the αC-domain with the BβN-domains in the presence of 200 μg/mL anti-Bβ1−21 mAb. (I) Paired bars representing cumulative probabilities of forces of >10 pN derived from panels A and D, B and E, and C and F. The dashed lines show the fitting with Gaussian curves to determine the position of each peak that corresponds to the most probable rupture force.

region and αC-domain with the BβN-domains, similar multimode rupture force spectra in the range of 10−170 pN were detected with three peaks at 30−35, 70−80, and 115−125 pN that were fitted with the Gaussians (Figure 2A,B). The peaks had a decreasing probability of interaction with larger forces, and the cumulative probability of all meaningful rupture forces of >10 pN was as much as 82% for the αC region and 83% for the αC-domain (Table 1). By contrast, the αC-connector was significantly less reactive with the BβN-domains, with no characteristic peaks and the cumulative probability of forces of >10 pN equal to only 49% ($p < 0.01$) (Figure 2C and Table 1).

When we replaced the fibrinogen BβN-domains with the fibrin βN-domains (Figure 1H), the interactions of the αC region and αC-domain largely vanished and the cumulative binding probability dropped ~2-fold ($p < 0.01$) (Figure 2D,-2E and Table 1), while the interactions of the αC-connector remained unchanged (Figure 2F). The bar graph in Figure 2I clearly shows that removal of FpB from the BβN-domains significantly reduced the binding probability of the αC region and αC-domain, suggesting that the interactions were mediated by FpB. At the same time, the reactivity of the αC-connector did not seem to depend on the presence of uncleaved FpB, indicating that the binding in the latter case was nonspecific, i.e., not mediated specifically by the N-terminal portions of the Bβ chains.

To verify the effect of FpB removal on the interactions of the αC region and αC-domain, we treated the surface-bound BβN-domains with thrombin (1 unit/mL, 37 °C, 1 h), which resulted in FpB cleavage and formation of the fibrin βN-domain right on the surface. The rupture force spectrum of the interactions of the thrombin-treated BβN-domains and

Table 1: Cumulative Binding Probability (all rupture forces > 10 pN) for Different Interacting Proteins[a]

interacting proteins	cumulative probability (%)	most probable rupture force (pN) peak 1	peak 2	peak 3	figure
αC region and Bβ N-domains	82 ± 21	33 ± 10	73 ± 16	124 ± 27	2A
αC-domain and Bβ N-domains	83 ± 19	31 ± 11	78 ± 8	115 ± 15	2B
αC-connector and Bβ N-domains	49 ± 13	no peak	no peak	no peak	2C
αC region and β N-domains	50 ± 12	no peak	no peak	no peak	2D
αC-domain and β N-domains	41 ± 6	no peak	no peak	no peak	2E
αC-connector and β N-domains	48 ± 6	no peak	no peak	no peak	2F
αC-domain and [Bβ N-domains with thrombin]	52 ± 11	no peak	no peak	no peak	2G
αC-domain and [Bβ N-domains with anti-Bβ1−21 mAb]	29 ± 6	no peak	no peak	no peak	2H
αC-domain and Bβ N-domains at a 1/10 surface density	35 ± 5	no peak	no peak	no peak	not shown
αC-domain at a 1/10 surface density and Bβ N-domains	26 ± 7	no peak	no peak	no peak	not shown
αC region and NDSK	88 ± 17	44 ± 13	no peak	no peak	3A
αC region and desA-NDSK	59 ± 9	41 ± 22	no peak	no peak	3B
αC region and desAB-NDSK	15 ± 4	no peak	no peak	no peak	3C
αC-domain and NDSK	89 ± 22	52 ± 17	no peak	no peak	3D
αC-domain and [NDSK with anti-Bβ1−21 mAb]	56 ± 12	no peak	no peak	no peak	not shown
αC-domain and desA-NDSK	71 ± 14	34 ± 17	no peak	no peak	3E
αC-domain and [desA-NDSK with anti-Bβ1−21 mAb]	26 ± 11	no peak	no peak	no peak	3F
αC-domain and desAB-NDSK	18 ± 5	no peak	no peak	no peak	not shown
αC region and αC region	62 ± 10	19 ± 3	36 ± 2	48 ± 2	4A
αC region and αC-domain	63 ± 12	17 ± 5	36 ± 2	49 ± 2	4B
αC region and αC-connector	26 ± 6	31 ± 6	no peak	no peak	4C
αC-domain and αC-connector	31 ± 7	25 ± 3	no peak	no peak	4D
αC-connector and αC-connector	27 ± 5	no peak	no peak	no peak	4E
αC-domain and BSA (negative control)	16 ± 4	no peak	no peak	no peak	4F
αC region and BSA (negative control)	21 ± 6	no peak	no peak	no peak	not shown

[a] Values are expressed as means ± the standard deviation.

the αC region (Figure 2G) appeared as a broad range of forces without well-defined peaks observed in Figure 2A and resulted in a significant reduction in binding probability (from 82 to 52%; $p < 0.01$). The mAb against the N-terminal portion of the Bβ chain (residues 1−21) caused an even more profound inhibitory effect on the αC−Bβ N interactions with a binding probability of 29% (Figure 2H and Table 1), further confirming that the interactions with the αC-domain were mediated by the N-terminal portions of the Bβ chains. When the surface density of the Bβ N-domain or the αC-domain was reduced 10-fold, the cumulative binding probability dropped to 35 and 26%, respectively (Table 1), thus providing additional evidence of the specificity of interactions between the αC- and Bβ N-domains.

Interactions of the αC Region and αC-Domain with NDSK. To check whether the binding mediated by the N-terminal portion of the Bβ chain was limited to the specific properties of the $(B\beta 1-66)_2$ fragment, we repeated the binding experiment with different forms of the N-terminal disulfide knot (NDSK), comprising the central part of fibrin(ogen) (Figure 1D−F). Binding of the αC region fragment and its active subfragment, αC-domain, was examined for three types of NDSK fragments that differed in their fibrinopeptide composition. Both FpA and FpB were intact in the NDSK (Figure 1D); only FpA was missing in desA-NDSK (Figure 1E), and both FpA and FpB were missing in desAB-NDSK (Figure 1F). For the interactions of the NDSK fragment with the αC region, a relatively sharp and prominent peak was observed with the most probable rupture forces at 44 ± 13 pN and higher forces of decreasing probability up to 150 pN. The overall reactivity of the proteins was high, and the cumulative binding probability reached 88% (Figure 3A and Table 1). The interactions of the αC region with desA-NDSK (Figure 3B) were much less pronounced compared to those of the NDSK (Figure 3A) with the cumulative binding probability of only 59% ($p < 0.01$), indicating that the N-terminal portions of the Aα chains are also involved in the binding with the αC region. Despite the reduction in the overall binding probability, a minor peak remained at 41 ± 22 pN (Figure 3B, dashed line), similar to the one resulting from the interactions of the αC region with NDSK (Figure 3A, dashed line). The removal of FpB in addition to FpA caused almost complete abrogation of the interactions of desAB-NDSK with the αC region (Figure 3C). The range of rupture forces significantly diminished to 10−90 pN, and the cumulative probability for these interactions dropped to 15%, a value similar to that for the nonspecific background interactions between the αC region and BSA (Table 1).

In accordance with the behavior of the αC region, the αC-domain also interacted with the NDSK readily, producing a wide range of forces from 10 to 170 pN, which could be very roughly segregated into two peaks centered at 52 ± 17 and 128 ± 26 pN (Figure 3D, dashed line). As shown for the αC region, the αC-domain was reactive with desA-NDSK (Figure 3E); however, the cumulative probability was somewhat lower than with the NDSK (71% vs 89%; $p < 0.05$). The moderate peak centered at 34 ± 17 pN could be revealed after fitting analysis, suggesting that the cleavage of FpA only partially weakened the interactions of NDSK with the αC-domain. Accordingly, the mAb against Bβ1−21 did not completely abrogate the interactions between the αC-domain and NDSK with the cumulative probability remaining at 56% (Table 1), far above those of the nonspecific background, indicating that the blocked N-terminal portions of the Bβ chains comprise only a part of the interaction site(s) for the αC-domain. By contrast, the inhibition of binding between the αC-domain and desA-NDSK with the anti-Bβ1−21 mAb was almost complete (Figure 3F), confirming the important contribution of the

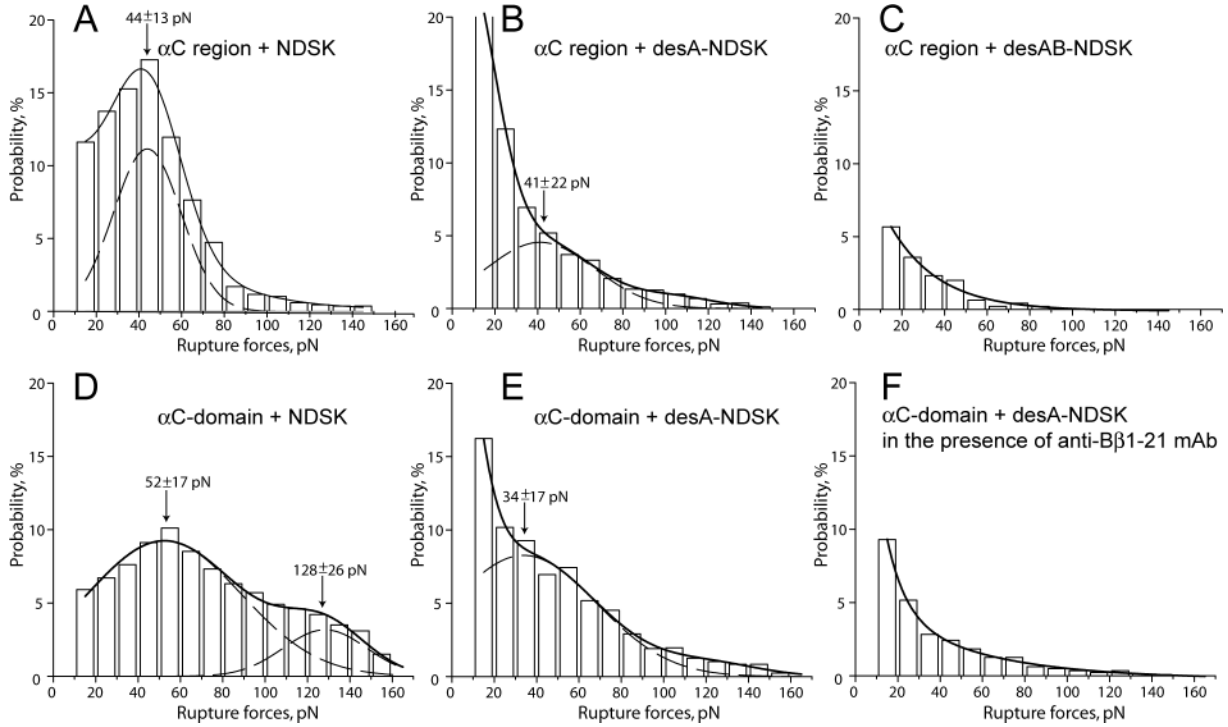

FIGURE 3: Panel of rupture force histograms demonstrating interactions of the recombinant αC region and αC-domain with various NDSK fragments corresponding to the central E region of fibrin(ogen). (A−C) Interactions of the αC region with NDSK, desA-NDSK, and desAB-NDSK, respectively. (D and E) Interactions of the αC-domain with NDSK and desA-NDSK, respectively. (F) Same as panel E, but in the presence of 200 μg/mL anti-Bβ1−21 mAb. The dashed lines show the fitting with Gaussian curves to determine the position of each peak that corresponds to the most probable rupture force.

N-terminal portions of the Bβ chains to the reactivity of NDSK with the αC-domain. The removal of FpB from desA-NDSK caused abrogation of the interactions of desAB-NDSK with the αC-domain (Table 1), as it did with the αC region. When the histograms depicted in Figure 3 and the data shown in Table 1 are compared, it is clear that the presence of both FpA and FpB was important for the interaction of the NDSK fragments with the αC region and αC-domain.

Interactions of the αC Region, αC-Domain, and αC-Connector with Each Other. To determine directly whether the αC region and its constituents, the αC-domain and αC-connector, can bind to each other, they were allowed to interact in different combinations. The pedestal-bound αC region reacted with the αC region coupled to a bead (Figure 4A); similarly, the pedestal-bound αC-domain reacted with the αC-domain coupled to a bead (Figure 4B). Both types of interactions produced similar rupture force spectra ranging from 10 to 65 pN with three peaks centered at ~20, 40, and 50 pN. The cumulative probabilities of those interactions were very similar, 62 and 63% for the αC-domain and αC-connector, respectively (Table 1). The probabilities were, however, significantly smaller ($p < 0.05$) than those observed for the interactions of the αC region and αC-domain with the BβN-domains and NDSK, despite comparable surface densities of the reacting proteins. The αC region and αC-domain both were poorly reactive with the αC-connector as inferred from the relatively low binding probabilities (26 and 31%, respectively); however, they formed moderate peaks of rupture forces at ~25−30 pN, indicating that the proteins were not fully inert (Figure 4C,D and Table 1). When the αC-connector was exposed to itself, the interactions formed a decreasing spectrum of rupture forces without any peaks and with a binding probability of 27% (Figure 4E), characteristic of the nonspecific protein−protein interactions.

DISCUSSION

The long-standing interest in the role of the C-terminal parts of the fibrinogen Aα chains, termed "αC-domains", in fibrin polymerization (*6*, *8*, *15*−*19*, *22*, *26*, *33*, *35*, *36*, *38*−*40*, *59*−*61*) has led to the current notion that the αC-domains are important participants of fibrin clot formation, although this is still controversial (*42*). There is evidence that the αC-domains accelerate fibrin polymerization and make the ultimate clot structure more stable, stiff, and resistant to fibrinolysis (*32*). It has been proposed that in fibrinogen the αC-domains interact intramolecularly with each other and with the central region, and during fibrin assembly, the αC-domains switch from intra- to intermolecular interaction, thus promoting lateral aggregation of protofibrils (*6*, *17*). This hypothesis is based largely on the indirect evidence obtained by differential scanning calorimetry (*59*, *60*) and transmission electron microscopy (*19*, *33*, *61*−*63*), demonstrating that in fibrinogen a pair of the αC-domains shows up as a globular particle near the central region, while in fibrin monomer they extend away from the backbone, forming two separate appendages. Many other experiments that utilized heterogeneous fibrin(ogen) degradation products or heterozygous dysfibrinogens (*6*) examine the αC-mediated interactions far less directly, making interpretation difficult and sometimes ambiguous. Therefore, the ability of the αC-domains to form specific associations still has been a matter of debate (*42*). In this study, for the first time, we directly observed and quantified the bimolecular interactions between recombinant fibrin(ogen) fragments containing the C-terminal parts of the Aα chains and

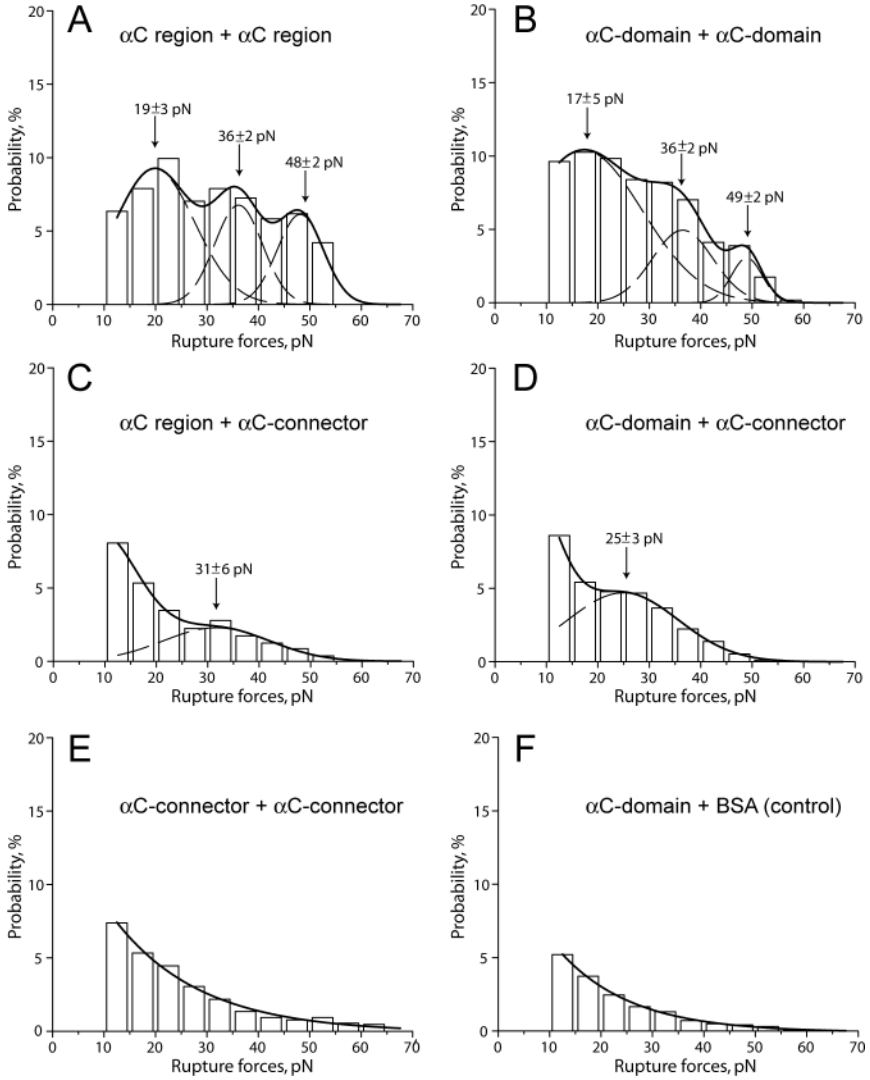

FIGURE 4: Panel of rupture force histograms demonstrating interactions of the αC region and its subfragments, αC-domain and αC-connector. (A) Interactions of the pedestal-bound αC region with the αC region coupled to a bead. (B) Pedestal-bound αC-domain with the αC-domain coupled to a bead. (C−E) Pedestal-bound αC region, αC-domain, and αC-connector with the αC-connector coupled to a bead, respectively. (F) Pedestal-bound αC-domain with the BSA-coated bead (negative control). The dashed lines show the fitting with Gaussian curves to determine the position of each peak that corresponds to the most probable rupture force.

the N-terminal portions of the Bβ chains, which reproduce the intramolecular associations of the αC-domains with the central part of the fibrinogen molecule and between each other. The results clearly show that there are specific interactions between the αC-domains and the central E region, which are partially reduced after cleavage of FpA and are fully abrogated upon FpB removal. In addition, the αC-domains form relatively weak homomeric associations, which are still stronger and more stable than the nonspecific background protein−protein interactions.

Although the whole αC region (Aα221−610) is reactive with the fragments derived from the fibrinogen E region, its binding capacity is largely determined by the relatively compact C-terminal portion, the αC-domain (Aα392−610), but not by the unstructured N-terminal αC-connector (Aα221−391). The αC region and αC-domain fragments both had remarkable and similar rupture force profiles with (Bβ1−66)$_2$ (Figure 2A,B) and NDSK (Figure 3A,B,D,E), while the αC-connector was significantly less reactive and displayed a qualitatively different behavior, showing rupture force profiles of lower cumulative probability (Table 1) without well-defined force peaks (Figure 2C,F). The overall force profile with an exponentially decreasing binding probability with larger forces, observed for the αC-connector, is characteristic of nonspecific background interactions (*45*, *64*). In addition, the reactivity of the αC-connector, unlike the αC region and αC-domain, was independent of the presence or absence of FpB in the BβN- or βN-domains (Figure 2C,F,I), indicating that the binding was not mediated specifically by the N-terminal portions of the Bβ chains and rather reflected nonspecific protein−protein interactions. Therefore, it is the αC-domain, but not the αC-connector, that serves as the reactive part of the αC region and is directly involved in the molecular interactions with the BβN-domains.

It was hypothesized that intramolecular interactions between the αC-domains and the central E region of fibrinogen were mediated by the N-terminal portions of the Bβ chains, including FpB (*19*). This assumption was tested and proved in this paper by direct exposure of the αC regions and αC-domains to the recombinant (Bβ1−66)$_2$ fragment mimicking the dimeric arrangement of the BβN-domains in fibrinogen. Both the αC regions and αC-domains readily reacted with (Bβ1−66)$_2$, producing a multimode rupture force spectrum (Figure 2A,B). These interactions vanished when this BβN-

domain-containing fragment was replaced with the $(\beta 15-66)_2$ fragment, containing two βN-domains (Figure 2D,E,I and Table 1). In addition, the interactions of the αC regions and αC-domains with $(B\beta 1-66)_2$ could be abrogated by direct cleavage of FpB by thrombin on the surface (Figure 2G) or blocking the N-terminal portions of the Bβ chains by the anti-Bβ1−21 mAb (Figure 2H). The susceptibility of the interactions to the presence or absence of exposed FpB indicates that the binding is specifically mediated by the N-terminal portions (residues 1−14) of the Bβ chains corresponding to FpB.

When $(B\beta 1-66)_2$ and $(\beta 15-66)_2$ were replaced with the NDSK fragments, which represent larger and more complex parts of the fibrin(ogen) central E region, the critical importance of FpB for binding with the αC-domains has been generally confirmed. In addition, it was found that the cleavage of FpA from NDSK, resulting in formation of desA-NDSK, partially weakened the ability of the αC regions and αC-domains to bind the isolated central E region (Figure 3A,B,D,E). Further cleavage of FpB from desA-NDSK, resulting in formation of desAB-NDSK, precluded binding to the αC regions (Figure 3C), as did the treatment of desA-NDSK with the anti-Bβ1−21 mAb (Figure 3F). These findings indicate that, in addition to FpB, the N-terminal portions of the Aα chains are also involved in the intramolecular interactions between the αC-domains and the central E region of fibrinogen. It should be noted that the cleavage of FpA itself does not seem to be sufficient for dissociation of the αC-domains from the central E region, as revealed by the previous electron microscopy analysis of desA- and desAB-fibrin (*33*). Thus, the FpB-mediated interactions appear to be critical for formation and maintaining of the intramolecular complex between the αC-domains and the central E domain in fibrinogen, while the FpA−αC interactions are likely to reinforce this complex and contribute to its stability.

Detailed analysis of the rupture force spectra enables us to quantify the strength of interactions at the single-molecule level. There are several indirect arguments favoring the idea that the three decreasing peaks of rupture force histograms in panels A and B of Figure 2 are indicative of the single, double, and triple αC−BβN binding, respectively. First, the maximum values of the weak (20−40 pN), intermediate (50−90 pN), and strong (100−150 pN) force peaks are roughly quantized, as would be predicted if they represent multiples of the bimolecular interactions (*65*). Second, the observed decreasing peak areas generally correspond to statistically predicted relative probabilities of the single, double, and triple molecular interactions. Third, the stronger forces are more susceptible to the inhibitory effects of FpB cleavage and the mAb treatment (Figures 2 and 3), which is consistent with the assumption that the stronger forces reflect multiple interactions and, therefore, disappear first. Fourth, the high incidence of multiple intermolecular interactions is confirmed by the relatively common occurrence of stepwise detachment of the interacting surfaces (10−20%). Taken together, these considerations suggest that the binding strength of the individual αC−BβN interactions represented by the weakest peaks in the force spectra should be ∼20−40 pN.

The hypothesized ability of the αC-domains to switch from intra- to intermolecular interaction during fibrin assembly implies that they bind each other specifically. This possibility was proved earlier by the fact that αC regions form homopolymers mimicking the arrangement of the αC-domains in fibrin (*33*, *39*), although the bimolecular binding between the isolated αC regions and/or its constituent parts has never been demonstrated. Our data clearly show that the αC regions do interact with each other at the single-molecule level and that the binding is mostly mediated by the αC-domains rather than the αC-connectors (Figure 4 and Table 1). The rupture force histograms produced by the αC−αC interactions differ from αC−BβN binding in two respects; first, they are significantly weaker (<60 and <160 pN, respectively) and, second, they seem to be more heterogeneous since the areas of the first, second, and third peaks are not very different (Figure 4A). Although it is tempting to attribute the weakest peak in the force spectrum to single-molecule binding, with other peaks being multiples, the remarkable heterogeneity of the interactions does not allow that to be done unambiguously. The complexity of these peaks may reflect multiple binding sites involved in αC−αC interactions. Indeed, at least two different types of binding sites are necessary to yield the linear α polymers formed by the αC-domains (*6*). Therefore, we infer that the αC-domains can form relatively weak and unstable homomeric associations. In fibrinogen, these associations are reinforced by the interactions of the αC-domains with the central E region via FpA and FpB. In fibrin, the αC−αC interactions are reinforced by the covalent factor XIIIa-mediated cross-linking.

It is noteworthy that the interactions revealed in this study between the fragments corresponding to the αC-domain and αC-connector, although quite weak and infrequent (Figure 4D), still exceed the nonspecific background (Figure 4F). This suggests that they have a specific component and may reflect those occurring in fibrin. To speculate about a possible physiological role of these interactions, one should recollect that the reactive Lys and Gln residues involved in covalent cross-linking of αC regions are located exclusively in their αC-domains and αC-connectors, respectively (*38*). This implies that to form cross-linked α polymers in fibrin, factor XIIIa should cross-link the αC-domains and αC-connectors of the neighboring molecules. In this case, the noncovalent interactions between the αC-domains and αC-connectors may bring them together and provide the proper orientation of the cross-linking sites to facilitate the covalent cross-linking and thereby reinforcement of α polymers in fibrin.

In conclusion, these results confirm the existence of the intramolecular interactions in fibrinogen between the αC-domains and the central E region. They provide the first direct evidence that these interactions are mediated by fibrinopeptide B and that fibrinopeptide A is also involved. In addition, the specific interactions were demonstrated between two identical αC-domains and between the αC-domains and the αC-connectors. Taken together, these results support the intra- to intermolecular switch hypothesis and provide insight into various αC-mediated interactions in fibrinogen and fibrin.

REFERENCES

1. Weisel, J. W. (2005) Fibrinogen and fibrin, *Adv. Protein Chem. 70*, 247−299.
2. Mosesson, M. W. (2005) Fibrinogen and fibrin structure and functions, *J. Thromb. Haemostasis 3*, 1894−1904.

3. Blomback, B., Blomback, M., Henschen, A., Hessel, B., Iwanaga, S., and Woods, K. R. (1968) N-Terminal disulphide knot of human fibrinogen, *Nature 218*, 130−134.
4. Brown, J. H., Volkmann, N., Jun, G., Henschen-Edman, A. H., and Cohen, C. (2000) The crystal structure of modified bovine fibrinogen, *Proc. Natl. Acad. Sci. U.S.A. 97*, 85−90.
5. Yang, Z., Kollman, J. M., Pandi, L., and Doolittle, R. F. (2001) Crystal structure of native chicken fibrinogen at 2.7 Å resolution, *Biochemistry 40*, 12515−12523.
6. Weisel, J. W., and Medved, L. (2001) The structure and function of the αC domains of fibrinogen, *Ann. N.Y. Acad. Sci. 936*, 312−327.
7. Tsurupa, G., Tsonev, L., and Medved, L. (2002) Structural organization of the fibrin(ogen) αC-domain, *Biochemistry 41*, 6449−6459.
8. Burton, R. A., Tsurupa, G., Medved, L., and Tjandra, N. (2006) Identification of an ordered compact structure within the recombinant bovine fibrinogen αC-domain fragment by NMR, *Biochemistry 45*, 2257−2266.
9. Lewis, S. D., Shields, P. P., and Shafer, J. A. (1985) Characterization of the kinetic pathway for liberation of fibrinopeptides during assembly of fibrin, *J. Biol. Chem. 260*, 10192−10199.
10. Ruf, W., Bender, A., Lane, D. A., Preissner, K. T., Selmayr, E., and Muller-Berghaus, G. (1988) Thrombin-induced fibrinopeptide B release from normal and variant fibrinogens: Influence of inhibitors of fibrin polymerization, *Biochim. Biophys. Acta 965*, 169−175.
11. Weisel, J. W. (1986) Fibrin assembly. Lateral aggregation and the role of the two pairs of fibrinopeptides, *Biophys. J. 50*, 1079−1093.
12. Weisel, J. W., Veklich, Y., and Gorkun, O. (1993) The sequence of cleavage of fibrinopeptides from fibrinogen is important for protofibril formation and enhancement of lateral aggregation in fibrin clots, *J. Mol. Biol. 232*, 285−297.
13. Doolittle, R. F. (1984) Fibrinogen and fibrin, *Annu. Rev. Biochem. 53*, 195−229.
14. Ariens, R. A., Lai, T. S., Weisel, J. W., Greenberg, C. S., and Grant, P. J. (2002) Role of factor XIII in fibrin clot formation and effects of genetic polymorphisms, *Blood 100*, 743−754.
15. Mosesson, M. W., Alkjaersig, N., Sweet, B., and Sherry, S. (1967) Human fibrinogen of relatively high solubility. Comparative biophysical, biochemical, and biological studies with fibrinogen of lower solubility, *Biochemistry 6*, 3279−3287.
16. Holm, B., Brosstad, F., Kierulf, P., and Godal, H. C. (1985) Polymerization properties of two normally circulating fibrinogens, HMW and LMW. Evidence that the COOH-terminal end of the α-chain is of importance for fibrin polymerization, *Thromb. Res. 39*, 595−606.
17. Medved, L. V., Gorkun, O. V., Manyakov, V. F., and Belitser, V. A. (1985) The role of fibrinogen αC-domains in the fibrin assembly process, *FEBS Lett. 181*, 109−112.
18. Weisel, J. W., and Papsun, D. M. (1987) Involvement of the COOH-terminal portion of the α-chain of fibrin in the branching of fibers to form a clot, *Thromb. Res. 47*, 155−163.
19. Gorkun, O. V., Veklich, Y. I., Medved, L. V., Henschen, A. H., and Weisel, J. W. (1994) Role of the αC domains of fibrin in clot formation, *Biochemistry 33*, 6986−6997.
20. Koopman, J., Haverkate, F., Grimbergen, J., Egbring, R., and Lord, S. T. (1992) Fibrinogen Marburg: A homozygous case of dysfibrinogenemia, lacking amino acids Aα 461−610 (Lys 461 AAA → stop TAA), *Blood 80*, 1972−1979.
21. Koopman, J., Haverkate, F., Grimbergen, J., Lord, S. T., Mosesson, M. W., DiOrio, J. P., Siebenlist, K. S., Legrand, C., Soria, J., Soria, C., et al. (1993) Molecular basis for fibrinogen Dusart (Aα 554 Arg → Cys) and its association with abnormal fibrin polymerization and thrombophilia, *J. Clin. Invest. 91*, 1637−1643.
22. Siebenlist, K. R., Mosesson, M. W., DiOrio, J. P., Soria, J., Soria, C., and Caen, J. P. (1993) The polymerization of fibrinogen Dusart (Aα 554 Arg → Cys) after removal of carboxy terminal regions of the Aα-chains, *Blood Coagulation Fibrinolysis 4*, 61−65.
23. Wada, Y., and Lord, S. T. (1994) A correlation between thrombotic disease and a specific fibrinogen abnormality (Aα 554 Arg → Cys) in two unrelated kindred, Dusart and Chapel Hill III, *Blood 84*, 3709−3714.
24. Furlan, M., Steinmann, C., Jungo, M., Bogli, C., Baudo, F., Redaelli, R., Fedeli, F., and Lammle, B. (1994) A frameshift mutation in Exon V of the Aα-chain gene leading to truncated Aα-chains in the homozygous dysfibrinogen Milano III, *J. Biol. Chem. 269*, 33129−33134.
25. Baradet, T. C., Haselgrove, J. C., and Weisel, J. W. (1995) Three-dimensional reconstruction of fibrin clot networks from stereoscopic intermediate voltage electron microscope images and analysis of branching, *Biophys. J. 68*, 1551−1560.
26. Collet, J. P., Woodhead, J. L., Soria, J., Soria, C., Mirshahi, M., Caen, J. P., and Weisel, J. W. (1996) Fibrinogen Dusart: Electron microscopy of molecules, fibers and clots, and viscoelastic properties of clots, *Biophys. J. 70*, 500−510.
27. Woodhead, J. L., Nagaswami, C., Matsuda, M., Arocha-Pinango, C. L., and Weisel, J. W. (1996) The ultrastructure of fibrinogen Caracas II molecules, fibers, and clots, *J. Biol. Chem. 271*, 4946−4953.
28. Ridgway, H. J., Brennan, S. O., Gibbons, S., and George, P. M. (1996) Fibrinogen Lincoln: A new truncated α chain variant with delayed clotting, *Br. J. Haematol. 93*, 177−184.
29. Ridgway, H. J., Brennan, S. O., Faed, J. M., and George, P. M. (1997) Fibrinogen Otago: A major α chain truncation associated with severe hypofibrinogenaemia and recurrent miscarriage, *Br. J. Haematol. 98*, 632−639.
30. Gorkun, O. V., Henschen-Edman, A. H., Ping, L. F., and Lord, S. T. (1998) Analysis of Aα251 fibrinogen: The αC domain has a role in polymerization, albeit more subtle than anticipated from the analogous proteolytic fragment X, *Biochemistry 37*, 15434−15441.
31. Vlietman, J. J., Verhage, J., Vos, H. L., van Wijk, R., Remijn, J. A., van Solinge, W. W., and Brus, F. (2002) Congenital afibrinogenaemia in a newborn infant due to a novel mutation in the fibrinogen Aα gene, *Br. J. Haematol. 119*, 282−283.
32. Collet, J. P., Moen, J. L., Veklich, Y. I., Gorkun, O. V., Lord, S. T., Montalescot, G., and Weisel, J. W. (2005) The αC domains of fibrinogen affect the structure of the fibrin clot, its physical properties, and its susceptibility to fibrinolysis, *Blood 106*, 3824−3830.
33. Veklich, Y. I., Gorkun, O. V., Medved, L. V., Nieuwenhuizen, W., and Weisel, J. W. (1993) Carboxyl-terminal portions of the α chains of fibrinogen and fibrin. Localization by electron microscopy and the effects of isolated αC fragments on polymerization, *J. Biol. Chem. 268*, 13577−13585.
34. Lau, H. K. (1993) Anticoagulant function of a 24-Kd fragment isolated from human fibrinogen Aα chains, *Blood 81*, 3277−3284.
35. Cierniewski, C. S., Plow, E. F., and Edgington, T. S. (1984) Conformation of the carboxy-terminal region of the Aα chain of fibrinogen as elucidated by immunochemical analyses, *Eur. J. Biochem. 141*, 489−496.
36. Cierniewski, C. S., and Budzynski, A. Z. (1992) Involvement of the α chain in fibrin clot formation. Effect of monoclonal antibodies, *Biochemistry 31*, 4248−4253.
37. Sobel, J. H., and Gawinowicz, M. A. (1996) Identification of the α chain lysine donor sites involved in factor XIIIa fibrin cross-linking, *J. Biol. Chem. 271*, 19288−19297.
38. Matsuka, Y. V., Medved, L. V., Migliorini, M. M., and Ingham, K. C. (1996) Factor XIIIa-catalyzed cross-linking of recombinant αC fragments of human fibrinogen, *Biochemistry 35*, 5810−5816.
39. Tsurupa, G., Veklich, Y., Hantgan, R., Belkin, A. M., Weisel, J. W., and Medved, L. (2004) Do the isolated fibrinogen αC-domains form ordered oligomers? *Biophys. Chem. 112*, 257−266.
40. Belkin, A. M., Tsurupa, G., Zemskov, E., Veklich, Y., Weisel, J. W., and Medved, L. (2005) Transglutaminase-mediated oligomerization of the fibrin(ogen) αC domains promotes integrin-dependent cell adhesion and signaling, *Blood 105*, 3561−3568.
41. Gorkun, O. V., Litvinov, R. I., Veklich, Y. I., and Weisel, J. W. (2006) Interactions mediated by the N-terminus of fibrinogen's Bβ chain, *Biochemistry 45*, 14843−14852.
42. Doolittle, R. F., and Kollman, J. M. (2006) Natively unfolded regions of the vertebrate fibrinogen molecule, *Proteins 63*, 391−397.
43. Ashkin, A. (1997) Optical trapping and manipulation of neutral particles using lasers, *Proc. Natl. Acad. Sci. U.S.A. 94*, 4852−4860.
44. Litvinov, R. I., Shuman, H., Bennett, J. S., and Weisel, J. W. (2002) Binding strength and activation state of single fibrinogen-integrin pairs on living cells, *Proc. Natl. Acad. Sci. U.S.A. 99*, 7426−7431.
45. Litvinov, R. I., Bennett, J. S., Weisel, J. W., and Shuman, H. (2005) Multi-step fibrinogen binding to the integrin αIIbβ3 detected using force spectroscopy, *Biophys. J. 89*, 2824−2834.
46. Litvinov, R. I., Gorkun, O. V., Owen, S. F., Shuman, H., and Weisel, J. W. (2005) Polymerization of fibrin: Specificity,

strength, and stability of knob-hole interactions studied at the single-molecule level, *Blood 106*, 2944−2951.
47. Litvinov, R. I., Gorkun, O. V., Galanakis, D. K., Yakovlev, S., Medved, L., Shuman, H., and Weisel, J. W. (2007) Polymerization of fibrin: Direct observation and quantification of individual B:b knob-hole interactions, *Blood 109*, 130−138.
48. Tsurupa, G., and Medved, L. (2001) Identification and characterization of novel tPA- and plasminogen-binding sites within fibrin(ogen) αC-domains, *Biochemistry 40*, 801−808.
49. Gorlatov, S., and Medved, L. (2002) Interaction of fibrin(ogen) with the endothelial cell receptor VE-cadherin: Mapping of the receptor-binding site in the NH_2-terminal portions of the fibrin β chains, *Biochemistry 41*, 4107−4116.
50. Kudryk, B., Rohoza, A., Ahadi, M., Chin, J., and Wiebe, M. E. (1983) A monoclonal antibody with ability to distinguish between NH_2-terminal fragments derived from fibrinogen and fibrin, *Mol. Immunol. 20*, 1191−1200.
51. Procyk, R., Kudryk, B., Callender, S., and Blomback, B. (1991) Accessibility of epitopes on fibrin clots and fibrinogen gels, *Blood 77*, 1469−1475.
52. Blomback, B., Hessel, B., Iwanaga, S., Reuterby, J., and Blomback, M. (1972) Primary structure of human fibrinogen and fibrin. I. Clevage of fibrinogen with cyanogen bromide. Isolation and characterization of NH_2-terminal fragments of the ("A") chain, *J. Biol. Chem. 247*, 1496−1512.
53. Blomback, B., Hessel, B., and Hogg, D. (1976) Disulfide bridges in NH_2-terminal part of human fibrinogen, *Thromb. Res. 8*, 639−658.
54. Ashkin, A. (1992) Forces of a single-beam gradient laser trap on a dielectric sphere in the ray optics regime, *Biophys. J. 61*, 569−582.
55. Svoboda, K., and Block, S. M. (1994) Biological applications of optical forces, *Annu. Rev. Biomol. Struct. 23*, 247−285.
56. Smith, S. B., Cui, Y., and Bustamante, C. (1996) Overstretching B-DNA: The elastic response of individual double-stranded and single-stranded DNA molecules, *Science 271*, 795−799.
57. Allersma, M. W., Gittes, F., deCastro, M. J., Stewart, R. J., and Schmidt, C. F. (1998) Two-dimensional tracking of ncd motility by back focal plane interferometry, *Biophys. J. 74*, 1074−1085.
58. Visscher, K., Gross, S. P., and Block, S. M. (1996) Construction of multiple-beam optical traps with nanometer-resolution position sensing, *IEEE J. Sel. Top. Quantum Electron. 2*, 1066−1076.
59. Privalov, P. L., and Medved, L. V. (1982) Domains in the fibrinogen molecule, *J. Mol. Biol. 159*, 665−683.
60. Medved, L. V., Gorkun, O. V., and Privalov, P. L. (1983) Structural organization of C-terminal parts of fibrinogen Aα-chains, *FEBS Lett. 160*, 291−295.
61. Erickson, H. P., and Fowler, W. E. (1983) Electron microscopy of fibrinogen, its plasmic fragments and small polymers, *Ann. N.Y. Acad. Sci. 408*, 146−163.
62. Mosesson, M. W., Hainfeld, J., Wall, J., and Haschemeyer, R. H. (1981) Identification and mass analysis of human fibrinogen molecules and their domains by scanning transmission electron microscopy, *J. Mol. Biol. 153*, 695−718.
63. Weisel, J. W., Stauffacher, C. V., Bullitt, E., and Cohen, C. (1985) A model for fibrinogen: Domains and sequence, *Science 230*, 1388−1391.
64. Leckband, D. E., Schmitt, F. J., Israelachvili, J. N., and Knoll, W. (1994) Direct force measurements of specific and nonspecific protein interactions, *Biochemistry 33*, 4611−4624.
65. Zhu, C., Long, M., Chesla, S. E., and Bongrand, P. (2002) Measuring receptor/ligand interaction at the single-bond level: Experimental and interpretative issues, *Ann. Biomed. Eng. 30*, 305−314.

BI700944J